Immersion lithography with numerical apertures above 2.0 using high index optical materials

Jianming Zhou[*a], Neal V. Lafferty[a], Bruce W. Smith,[a] John H. Burnett[b]
[a]Center for Nanolithography Research, Rochester Institute of Technology,
82 Lomb Memorial Drive, Rochester, NY 14623;
[b]NIST, 100 Bureau Dr., Gaithersburg, MD, USA 20899-8421

ABSTRACT

The progress of optical lithography has approached the sub-30 nm regime using 193nm excimer lasers as the exposure sources. To increase the numerical aperture (NA) further, many issues, especially those related to materials, need to be addressed. In this paper, we present the analytical and experimental results of oblique two-beam lithography with sapphire (Al_2O_3) as the optical material. At 193nm, the index of sapphire is 1.92 while the typical index of a photoresist is near 1.70. Classical theory predicts that, ignoring the absorbance in the photoresist, once the NA is greater than the photoresist refractive index, no energy will be transmitted across the sapphire/photoresist boundary due to total internal reflection. However, it can be shown that the absorbance in the resist prevents a "critical angle" and total internal reflection will not occur. Photoresist exposure can result even when NA is greater than the photoresist refractive index. The image profile is strongly affected by the real and imaginary parts of the photoresist refractive index. Optimization of photoresist optical properties is necessary for good image profile. Lutetium aluminum garnet ($Lu_3Al_5O_{12}$ or LuAG with an index 2.14 at 193 nm) is also investigated as an alternative lens material.

Keywords: immersion lithography, hyper-NA, total internal reflection, oblique angle

1. INTRODUCTION

Optical lithography has been the key technology driving the evolution of semiconductor industry. The advances in integrated circuits (IC) fabrication have demanded optical lithography with the ability of printing smaller CDs as well as other specifications as indicated by international technology roadmap of semiconductor (ITRS).[1] This trend will continue. Because the resolution of optical lithography is diffraction limited, a few other technologies have been proposed as alternatives to optical lithography. However, all of these candidates still have serious technical challenges. To utilize the numerous resources existing for optical lithography, interests in pushing the resolution limit of optical lithography will continue. The resolution limit of an optical lithography system is described by the Rayleigh's Criterion.[2] While it is hard to achieve smaller CD by reducing the illumination wavelength and the processing dependent factor, the CD can be reduced by increasing the numerical aperture (NA). NA is defined as $n\sin\theta$, where n is the refractive index (RI) of the medium and θ is the incident angle. Immersion lithography has enhanced the resolution limit of optical lithography by a factor of the RI of the immersion medium. However, the NA of an immersion lithography system is still limited by the indices of the lens material and the immersion fluid. To remove the resolution limits imposed by the fluid RI, an approach can be applied that eliminates the immersion fluid from the system and uses high RI optical materials for the last lens element. In this approach, the lens material is in intimate contact with the film stack, i.e. the lens is the immersion medium. A very small air gap exists between the lens and the film stack. This gap is estimated to be less than 15nm. This system enables us to study extreme high NA conditions with the materials that are available. High RI lens materials, such as Al_2O_3 (sapphire with RI = 1.92) and LuAG (lutetium aluminum garnet with RI = 2.14) offer the possibility of achieving NA of 1.7~2.1. The imaging mechanisms that allow the NA to be greater than the resist index will be discussed in this paper. We will also show that once the NA is close to the real part of the photoresist refractive index, the imaging profile is strongly related with the real and imaginary refractive index of the photoresist.

* Correspondence: jaz0485@rit.edu; web: www.rit.edu/lithography

2. HYPER-NA IMAGING APPARATUS

A two beam lithography system was built to perform the interferometric lithography at extremely oblique angles. The detailed setup is described in our previous publication.[3] A laser beam is expanded and TE polarized. A phase grating serves as a beam splitter. The 0^{th} order is blocked by a beam blocker. The 1^{st} and the -1^{st} diffraction orders are used as the interference waves. They are directed into a prism, and finally form a sinusoidal intensity distribution on the prism/photoresist interface. The turning mirrors, combined with the phase grating pitch, define the arrival angle θ on the wafer. On the image side, the effective NA is $n_{prism}\sin\theta$. By changing the impinging angle, the resultant pitch size can be calculated as

$$\Lambda = \lambda/(2n_{lens}\sin\theta) \tag{1}$$

Fused silica is widely used for 193nm lithography due to its excellent optical properties at this wavelength.[4] However, the RI of fused silica is only 1.56. To investigate lithography with extreme oblique angle in the photoresist, the NA needs to be close to the resist index, which is typically around 1.7. This NA is impossible for a fused silica lens. A few optical materials have refractive indices higher than the photoresist index. To be used as a lens material, the optical material should also satisfy a few other requirements, such as low absorbance, low birefringence, and low index inhomogeneity. Sapphire has a refractive index of 1.92 at 193nm, and it is transparent down to 180nm. The birefringence of a lens material needs to be less than 10^{-6}.[5] However, the birefringence of sapphire is 0.008.[6] When a linearly polarized beam propagates in a birefringent material, birefringence may induce depolarization.[7] Because of the hexagonal crystal structure of sapphire, it is easy to make an equilateral prism with it. For a sapphire prism, the principal axis is on z direction as shown in Figure 1. For TE polarized beam, the electric field is on z direction, i.e. the optical axis. For two beam interference, the wave propagates in the isotropic xy plane and no birefringence induced depolarization will happen.

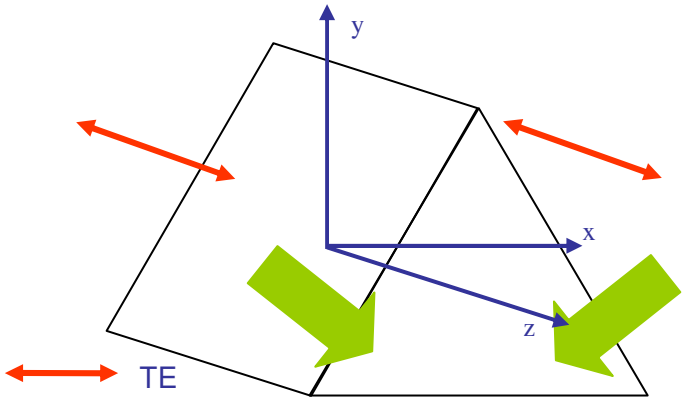

Figure 1. The direction of the incident wave electric field is on the principal axis of the lens material. Birefringence induced depolarization effect is avoided with this arrangement.

The films stack along with their refractive indices is illustrated in Figure 2. The lens element is made of sapphire. The topcoat is JSR TCX014, which prevents airborne contamination. JSR ARX2928JN is a positive chemically amplified resist (CAR). The bottom anti-reflective coating (BARC) is Brewer AR29A-8 which helps to reduce standing waves. The substrate is a silicon wafer. For this film stack, the lens and the topcoat are non-absorbing. Since the lens material has a higher refractive index than the topcoat, a critical angle exists.[8] Total internal reflection (TIR) results with an evanescent wave decaying from the interface when the incident angle in the lens is beyond critical. The evanescent wave does not propagate unless it is perturbed. For the film stack shown in Figure 2, the perturbation is achieved by the photoresist layer. The thickness of the topcoat is 40nm. The photoresist has a refractive index of 1.7-0.04i, so it can perturb the evanescent wave when the NA is less than 1.7. In fact, as we will explain in the following sections, because of the small absorbance of the photoresist, the effective refractive index of the photoresist is higher than the NA. The evanescent wave can be perturbed even when NA is greater than 1.7. The amplitude of the field at the topcoat/resist interface is dependant on the wavelength, the incidence angle, and the gap thickness.[3] Therefore, the NA of this system is not limited by the refractive index of the topcoat.

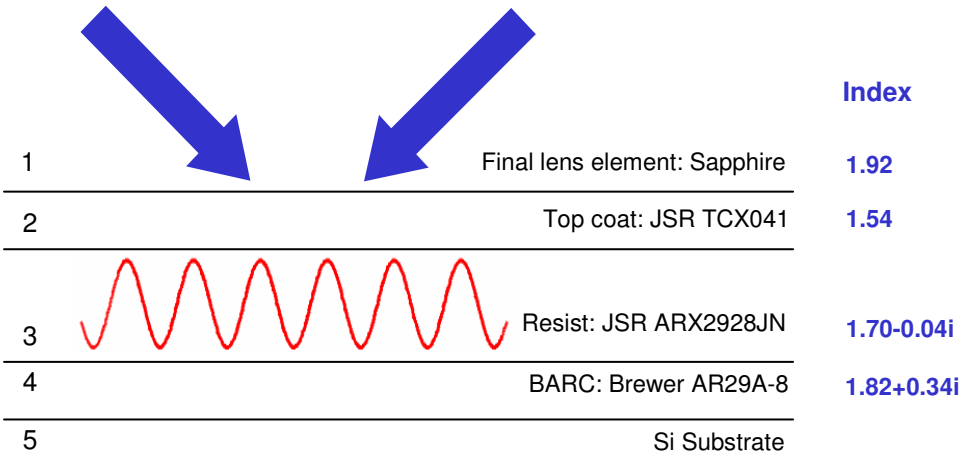

Figure 2. The lens is in contact with the photoresist stack.

3. HYPER-NA IMAGING RESULTS

Exposures with different numerical apertures were done with the apparatus described in the previous section. A few interesting phenomena were investigated when NA is above or near the photoresist index. Possible exposure with NA above 2.0 is also discussed in the next a few sections.

A. Conditions where NA exceeds the resist index

Wave refraction is well described by Descartes-Snell's law. The extinction coefficient of a photoresist is typically around 0.04 and it is small compared with the real part of photoresist index (~1.7). For typical calculations of wave refraction, the photoresist is approximated as non-absorbing material with refractive index n. The refracted angle in the second medium is

$$\theta_2 = \arcsin(NA/n) \tag{2}$$

Based on this assumption, when the NA is greater than n, imaging will not happen since all the energy will be reflected. However, 1.85 NA imaging with a half pitch of 26nm was achieved, as shown in Figure 3. Therefore, the non-absorbing approximation needs to be reconsidered.

The lens still can be approximated as a transparent material with refractive index n_1, the photoresist has a complex refractive index $\hat{n} = n - ik$. Using Descartes-Snell's law, the complex angle of refraction in the second medium θ_2 is

$$\hat{\theta}_2 = \arcsin(NA/\hat{n}) \tag{3}$$

The mathematical expression for θ_2 leads to a complex refracted angle [9] whereas the actual propagating angle is real. As illustrated in Figure 4,[10] assuming a plane wave $P_1P_2P_3$ is propagating from the first medium into the second medium, $P_1P_2P_3$ have constant phase and amplitude. Let the propagating angle in the second medium to be θ_2' and the effective RI of the second medium is n' (as we will see later, n' is not equal to n).

$$\frac{\sin\theta_1}{\sin\theta_2'} = \frac{n'}{n_1} \tag{4}$$

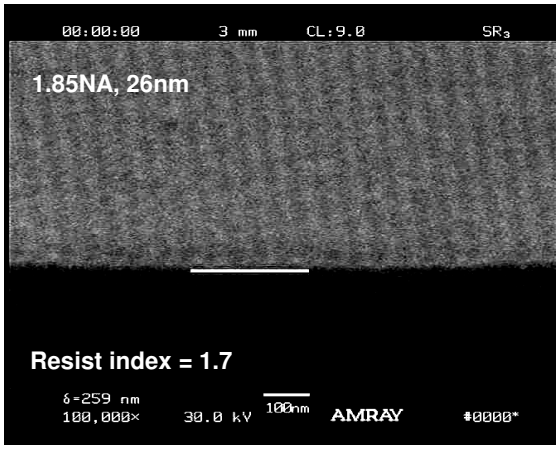

Figure 3. Imaging with 1.85NA, 26nm half pitch was achieved with sapphire prism.

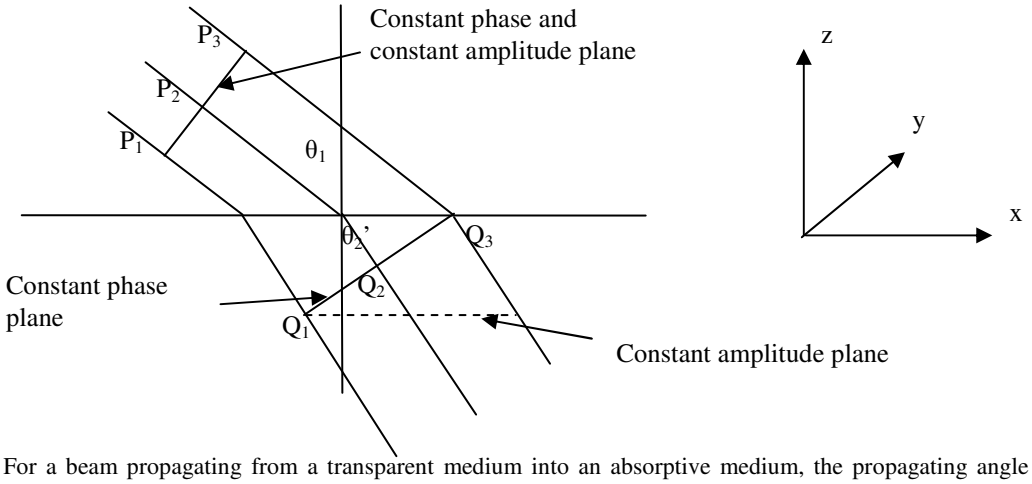

Figure 4. For a beam propagating from a transparent medium into an absorptive medium, the propagating angle in the second medium is a function of the extinction coefficient of the second medium.

In the second medium, $Q_1Q_2Q_3$ form a constant phase surface perpendicular to the propagating direction. If the second medium is non-absorptive, this surface is also a surface of constant amplitude. However, for absorptive material, the amplitude at different points on this surface is determined by the length of path. The surface of constant amplitude is the dashed line in Figure 4 and is parallel to the interface. The propagating direction is normal to the constant phase surface. The electric field propagating into the second medium is:

$$E_{2y} = A_{2y} \exp i\left\{\omega t - \vec{k} \cdot \vec{r}\right\} \tag{5}$$

Where A_{2y} is the wave amplitude, ω is the angular temporal frequency, t is time, $\vec{k}$ is the wave vector, and $\vec{r}$ is the position vector. We can rewrite equation (5) as:

$$E_{2y} = A_{2y} \exp i\omega\left\{t - \frac{n'}{c}\left(x\sin\theta_2' - z\cos\theta_2'\right) - \frac{ik'z}{c\cos\theta_2'}\right\} \tag{6}$$

where n' and k' are the effective RI and extinction coefficient of medium 2 and c is the speed of wave in vacuum. When E_{2y} is substituted into the usual wave equation,

$$\left(\frac{\partial^2}{\partial x^2}+\frac{\partial^2}{\partial y^2}+\frac{\partial^2}{\partial z^2}\right)E_{2y}+\left(\frac{\omega}{c}\right)^2\hat{n}^2E_{2y}=0 \tag{7}$$

we obtain

$$\left(-\frac{i\omega n'}{c}\sin\theta_2'\right)^2+\left(\frac{i\omega n'}{c}\cos\theta_2'+\frac{\omega k'}{c\cos\theta_2'}\right)^2E_y+\left(\frac{\omega}{c}\right)^2(n+ik)^2E_y=0 \tag{8}$$

By separating the real and imaginary components, we have

$$n'^2-\left(\frac{k'}{\cos\theta_2'}\right)^2=n^2-k^2 \text{ and}$$
$$n'k'=nk \tag{9}$$

From Equation (4) and (9), we can solve *n', k'* and θ_2':

$$n'=\left(\frac{n^2-k^2+NA^2+\sqrt{\left(n^2-k^2+NA^2\right)^2-4\left[\left(n^2-k^2\right)NA^2-n^2k^2\right]}}{2}\right)^{1/2}$$
$$k'=nk/n' \tag{10}$$
$$\theta_2'=\arcsin\left(NA/n'\right)$$

For the case of non-absorbing materials, i.e. k is zero, it can readily be shown that

$$n'=n \qquad \text{(NA<n)}$$
$$n'=NA \qquad \text{(NA>n)}$$
$$k'=0 \tag{11}$$
$$\theta_2'=\arcsin(NA/n)$$

This is simply Snell's law for non-absorbing material. We define the NA in the second medium as

$$NA=n'\sin\theta' \tag{12}$$

In this example the complex refractive index of the photoresist is 1.7-0.04i and the refractive index of the lens material is 1.92. The effective refractive index of the photoresist can be calculated from Equation 10 and is shown in Figure 5. The effective refractive index is still higher than the NA for different incident angle.

Figure 6 shows that the effective extinction coefficient slightly decreases with the incident angle θ_1. This is because the absorbance per unit distance is a constant, i.e.

$$\alpha=\frac{4\pi k}{\lambda}=\frac{4\pi nk}{\lambda_0}=\frac{4\pi n'k'}{\lambda_0} \tag{13}$$

where λ_0 is the wavelength in vacuum. Therefore, if the wavelength in the photoresist is λ_0/n', the effective extinction coefficient becomes nk/n' and decreases with NA. We define the effective absorbance along the z direction as

$$A_z = \alpha \frac{1}{\cos\theta'} \tag{14}$$

A_z indicates how the intensity drops along the z direction. When the refracted angle is large, then the effective absorbance is large. If the photoresist is approximated as non-absorbing material, the refracted angle θ can be calculated from Equation 2. Once the incident angle is beyond critical, θ becomes 90^o and the effective absorbance becomes infinity. Fortunately if we correct the approximation by taking the small absorbance into account, the actual refracted angle in the photoresist is θ' and never reaches 90^o. The effective absorbance along z direction is still a finite number. Figure 7 shows the difference of the corrected and uncorrected effective absorbance along the z direction, which essentially shows the difference between *1/cosθ'* and *1/cosθ.*

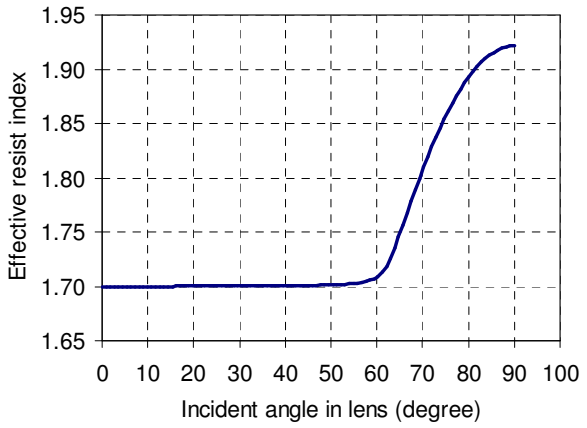

Figure 5. The effective refractive index of the photoresist is a function of the incident angle.

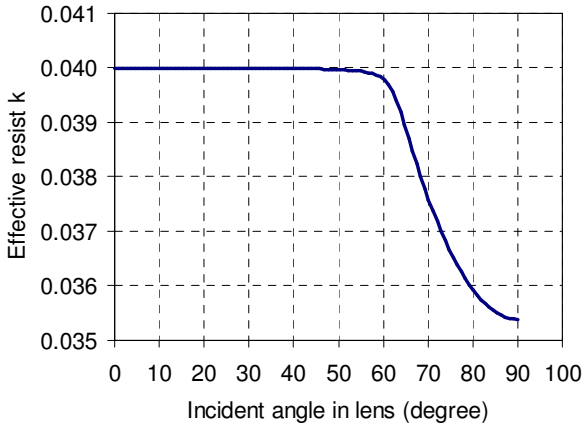

Figure 6. The effective extinction coefficient decreases with the incident angle.

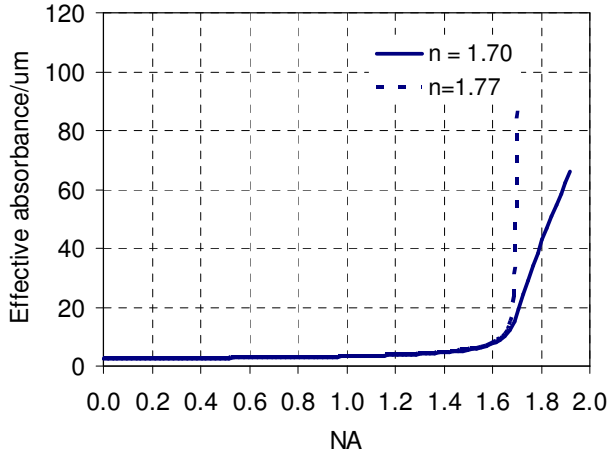

Figure 7. The effective absorbance along z direction A_z increases with NA. With non-absorbing approximation, the A_z becomes infinity once the incident angle is beyond critical. With correction, A_z is a finite number for any NA.

B. Conditions where NA is near the photoresist index

Figure 8 shows a series of exposure results with different NA's. The image profile degrades when the NA increases. The imaging becomes very difficult when the NA exceeds n. When NA = 1.6, the lines are clearly resolved. When NA = 1.75, the image depth is shallow. It becomes surface imaging with a few nanometers depth when NA = 1.82.

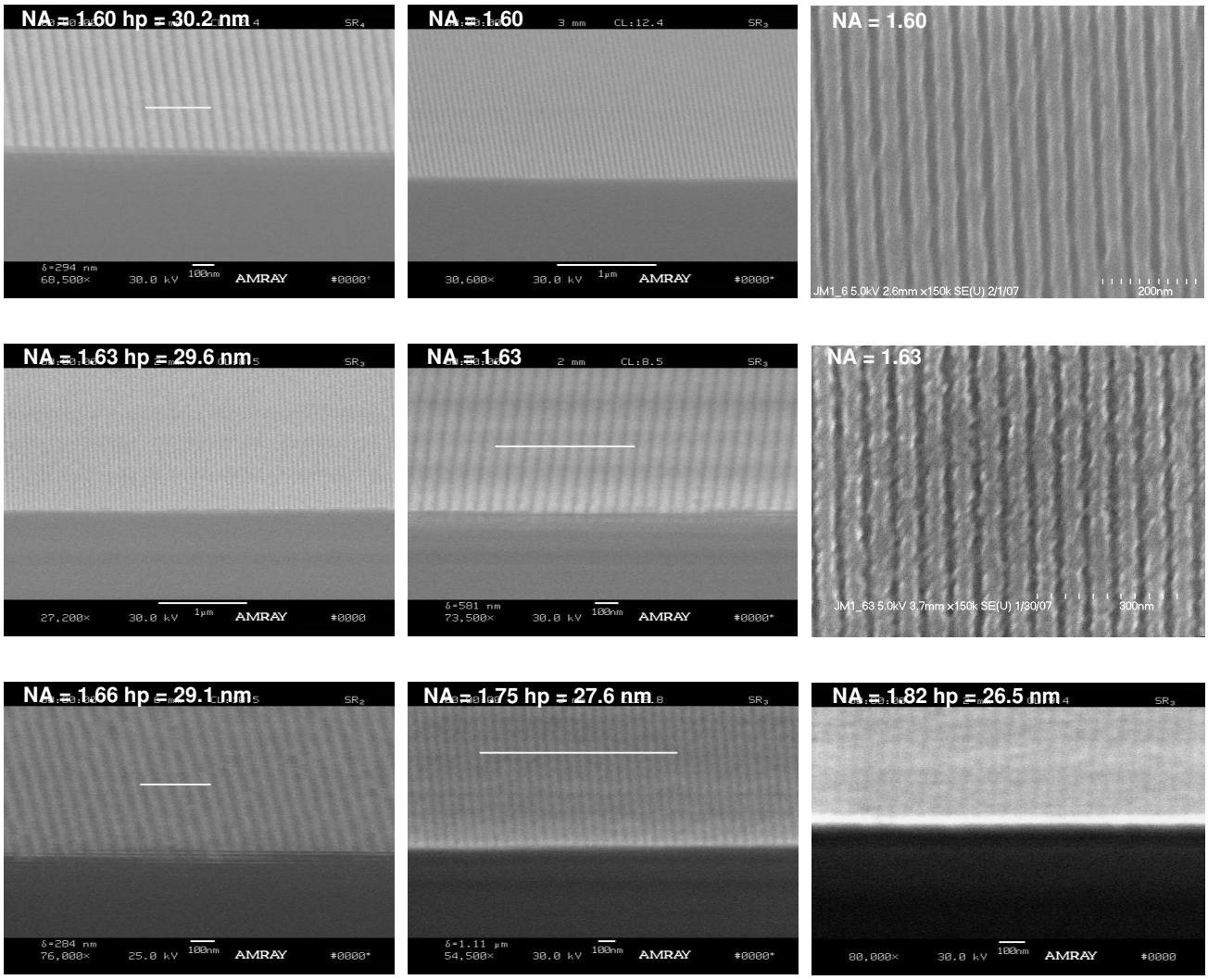

Figure 8. When NA is close to n, the image profile degrades with NA. The image depth decrease with NA and it becomes surface imaging when NA = 1.82.

The propagating angle in the photoresist is close to grazing angle for large NA imaging. The actual optical path of the beam in the photoresist is large even when the photoresists film is thin. As discussed in the previous section, the effective absorbance A_z is large for oblique angle. The intensity drops quickly along the z direction and the bottom of the resist may not be exposed while the top of the photoresist is over exposed. The oblique angle in the resist can be reduced by using a high index photoresist material. The A_z of the photoresist that we used is shown in Figure 9 a) along with the A_z of a hypothetical resist with n = 1.77 for comparison. A_z is reduced when a high index photoresist is used. The exposures were done with same BARC material. The BARC is not optimized for NA in this regime. It is difficult to achieve low reflection at the resist/BARC interface. The BARC thickness was chosen for minimum reflection for each NA, however for NA ~ 1.6, the reflection is about 10%. The reflected wave forms destructive node with the incident wave above the resist/BARC interface. This also reduces image depth. Figure 9 b) shows the minimum achievable reflection as NA changes. If a photoresist with n = 1.77 is used, the reflection can be reduced. Large amount of reflection at the lens/resist interface will be resulted due to the index mismatch at high NA. Part of the reflected energy will become flare. Large amount of flare will decrease the image modulation and makes the imaging to be difficult. Figure 9 c) shows the reflection reduction by using a high refractive index photoresist.

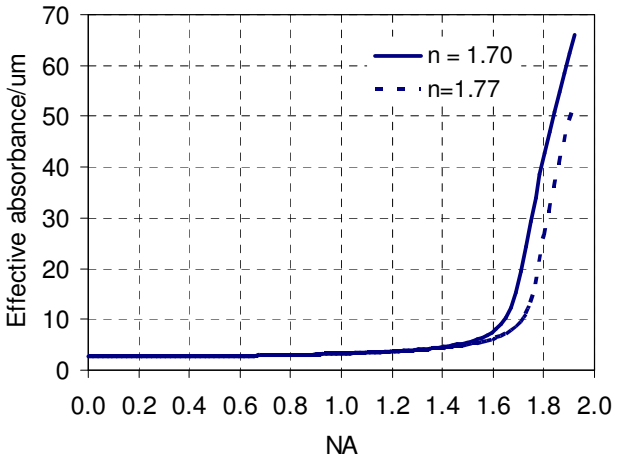

a)

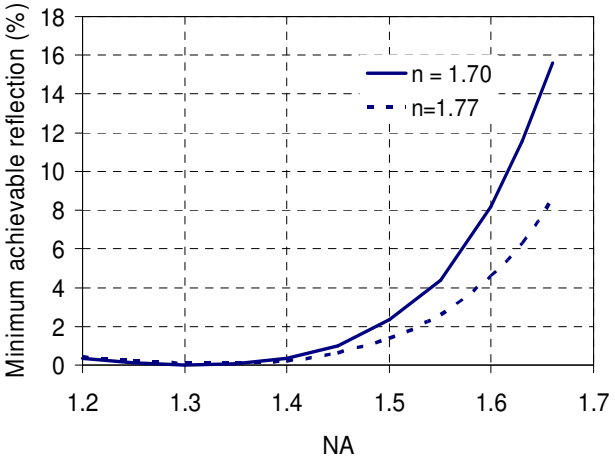

b)

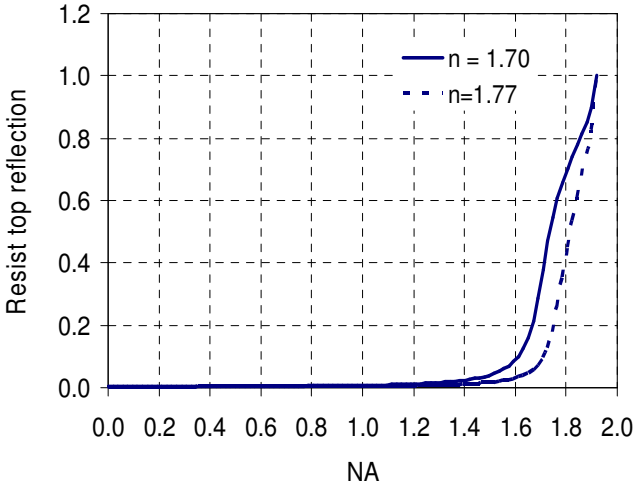

c)

Figure 9. a) The effective absorbance, the minimum achievable reflection at the resist/BARC interface and the reflection from the top of the photoresist can be reduced by using high index photoresist. a) The effective absorbance along the z direction becomes extremely large for imaging at very large oblique angle. b) It is difficult to achieve low reflection at very high NA. c) The large amount of the reflection from the lens/resist interface will increase flare and decrease image modulation.

C. Conditions where NA is above 2.0

Other than simple oxides, lutetium aluminum garnet (LuAG) is another candidate as high index lens material. The characteristics of LuAG are summarized in Table 1.[5] LuAG exists in cubic form and has a similar crystal structure to yttrium aluminum garnet (YAG) with yttrium atoms replaced by lutetium atoms. Garnet structure is complicated with eight units of $Lu_3Al_5O_{12}$ in one conventional unit cell. The detailed crystal structure of garnet is widely available in literature.[11,12] Because of its cubic crystal structure, LuAG has no structural birefringence like that of sapphire (though it still has a small spatial-dispersion-induced birefringence "intrinsic birefringence" of 30 nm/cm.[5]). This makes LuAG a possible candidate for hyper-NA lithography. The fabrication of LuAG prism is still underway. With LuAG, NA above 2.0 is possible.

Table 1. Summary of LuAG optical properties[5]

Material	n	$dn/d\lambda$ (cm^{-1})	dn/dT (10^{-5} K^{-1})	A_{10} (cm^{-1})	IBR (nm/cm)
LuAG	2.1435±0.0002	-0.0039±0.0001	6.1±0.3	3.7	30.1±1.4

4. CONCLUSION

In this work, the mechanism of lithography with NA beyond the refractive index of the photoresist was investigated. The small absorbance of the photoresist can increase the effective refractive index of the resist and makes imaging possible. The extinction coefficient is very important for imaging at oblique angles. To accurately model the wave propagation in the photoresist at oblique angle, the small absorbance of photoresist must be considered. However, the image profile is poor when the NA is approaching n due to the index mismatch of the lens/resist and the resist/BARC. The image profile can be improved by using high refractive index photoresist because it can reduce the effective absorbance along z direction and the reflection at the resist/BARC interface. Fabrication of a LuAG prism has begun, and imaging with NA above 2.0 will be investigated once the LuAG prism is ready.

ACKNOWLEDGEMENTS

The authors acknowledge SRC, Intel, Corning Tropel, JSR, Brewer Science, ASML, IBM, Exitech, International SEMATECH, DARPA/AFRL, ARCH, Photronics, KLA-Tencor, and TOK for their generous support of this research.

REFERENCES

1. "International technology roadmap for semiconductors 2006 update, Lithography," (2006), http://www.itrs.net/Links/2006Update/FinalToPost/08_Lithography2006Update.pdf.
2. J. R. Sheats and B. W. Smith, Microlithography: Science and Technology. Marcel Dekker, New York, 1998.
3. B. W. Smith, Y. Fan, J. Zhou, N. V. Lafferty, A. Estroff, “Evanescent wave imaging in optical lithography”, Proc. SPIE Optical Microlithography, vol. 6154 (2006).
4. B. W. Smith, Excimer Laser Microlithography at 193 Nm, 1994.
5. J. H. Burnett, S. G. Kaplan, E. L. Shirley, D. Horowitz, W. Clauss, A. Grenville, C. V. Peski, “High-index optical materials for 193-nm immersion lithography”, Proc. SPIE Optical Microlithography, vol. 6154 (2006).
6. http://www.insaco.com/MatPages/sapphire.asp
7. E. A. Saleh and M. C. Teich, Fundamentals of Photonics, Wiley, New York, 1991.
8. Hecht, Optics, Addison-Wesley, Reading, Mass., 2002.
9. P. E. Ciddor, "Explicit evaluation of the complex angle of refraction in an absorbing medium", Indian Journal of Pure Applied Physics v20, n5, 397(1982).
10. R. W. Ditchburn, Light, Interscience Publishers, New York, 1963.
11. R. W. G. Wyckoff, Crystal Structures, Interscience Publishers, New York, 1963.
12. H. Li, X. Liu, L. Huang, "Fabrication of Transparent Cerium-Doped Lutetium Aluminum Garnet (LuAG:Ce) Ceramics by a Solid-State Reaction Method" Journal of the American Ceramic Society, v 88, n11, 3226 (2005).